Progress In Electromagnetics Research Letters, Vol. 34, 111–122, 2012

PREDICTION OF MULTIPLE MAGNETIC DIPOLE MODEL PARAMETERS FROM NEAR FIELD MEASUREMENTS EMPLOYING STOCHASTIC ALGORITHMS

N. C. Kapsalis*, **S.-D. J. Kakarakis, and C. N. Capsalis**

National Technical University of Athens, Greece

Abstract—In this paper, the problem of predicting far field magnitude from near field measurements of an equipment under test (EUT) is studied. Firstly, a multiple magnetic dipole model is developed to simulate the magnetic behavior of the EUT. The parameters of the model (dipoles positions and magnetic moments) are calculated using the values of the near field applying the Particle Swarm Optimization (PSO) algorithm. For the evaluation of the method, extended simulations were conducted, producing theoretical values and distorting them with noise, and then the developed algorithm was used to create the proper model. Finally, the theoretical results are compared to the field assessments the proper models produced.

1. INTRODUCTION

The problem of searching magnetic sources from locally measured magnetic fields belongs to the category of inverse electromagnetic problems and covers many applications [1–5]. Magnetic cleanliness is crucial in space missions. Measuring equipment, placed on spacecrafts and measuring magnetic fields, operates in a particularly magnetic environment. The magnetic fields that these missions focus on are usually weak, so the magnetometers must be placed in "clean" specification points, where the total magnetic field of the spacecraft lies between 0.1–1 nT [1].

In order to estimate the magnetic behavior of equipment placed in spacecrafts, accurate models and new methods must be considered. Such models have been developed in the past [1], and they are based on the development of multiple magnetic dipole models (MDM). The

Received 9 March 2012, Accepted 2 May 2012, Scheduled 4 September 2012

* Corresponding author: Nikolaos C. Kapsalis (ncapsalis@gmail.com).

parameters of the models (position, magnetic torque) are estimated taking into account of measurements in coil facilities [1]. Based on these measurements, algorithms of renowned capability are employed to solve the inverse problem [4, 6].

The MDM technique has been employed in many applications such as near field analysis in the antennas field [7], electrocardiography simulation [8] and the representation of electromagnetic emissions of an Integrated Circuit [9].

Alternative techniques for deterministic methods are nowadays available to efficiently find global optima. In [10, 11] metaheuristic methods have been employed to study electromagnetic radiation problems. Stochastic search techniques start to be widely used with their main advantage that they do not need assumption on objective function's properties and do not need identification of a starting point. Therefore, they are more robust than deterministic methods. Their main disadvantage is that due to the high number of function evaluations that they are using, they need increased computer power. One of these randomized methods is called Particle Swarm Optimization (PSO).

The present work employs a PSO approach to implement an algorithm in order to produce a set of magnetic dipoles that have the biggest probability to predict the magnetic field produced by a specific Equipment Under Test (EUT). PSO is a stochastic optimization method, inspired by biology and used widely for a variety of problems, such as antenna design [12–14] and resource allocation [15].

In order to evaluate the proposed method, initially a theoretical model — composed by a number of magnetic dipoles randomly positioned — is assumed. Based on that model, the theoretical field values at the positions of possible measurements locations are produced. These locations usually form a circle centered to the EUT to be modeled. In this way, the theoretical values of the measurements are produced.

Afterwards, these theoretical values are distorted with noise in order to create a set of so-called measurements with a predefined percentage of distortion which may vary from 1% to 5%.

The so-called measurements are then used to predict both the positions and the magnetic moments of the set of dipoles composing the model. Finally, as an evaluation criterion, the root mean square (rms) error between the magnetic field values produced by the model and the so-called measurements is calculated.

The paper is organized as follows. Section 2 includes the theoretical background, while in Section 3 the numerical results are presented followed by the conclusions of the process.

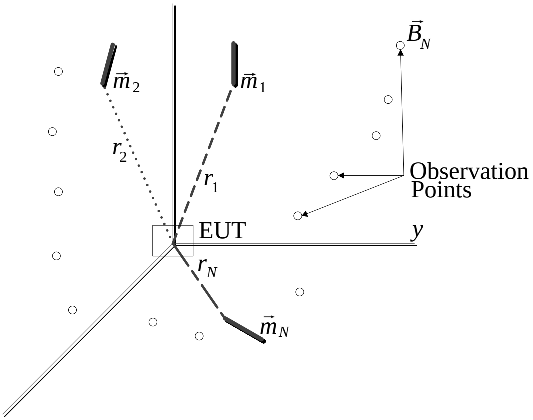

Figure 1. Problem depiction.

2. MATHEMATICAL FORMULATION

2.1. Background

In Figure 1, geometry of the problem under consideration is depicted.

The EUT is assumed to be positioned at the point with coordinates (0, 0, 0). The EUTs magnetic behavior may be modeled by a set of magnetic dipoles. These dipoles are positioned at (x_i, y_i, z_i), $i = 1, 2, \ldots, N$, with magnetic moments

$$\vec{m}_i = mx_i \cdot \hat{x} + my_i \cdot \hat{y} + mz_i \cdot \hat{z} \tag{1}$$

The M observation points are positioned at (x_{0j}, y_{0j}, z_{0j}), $j = 1, 2, \ldots, M$.

The magnetic field of dipole i at the observation point j expressed as the superposition of B_x, B_y, B_z

$$\vec{B}_{ij} = Bx_{ij} \cdot \hat{x} + By_{ij} \cdot \hat{y} + Bz_{ij} \cdot \hat{z} \tag{2}$$

where

$$Bx_{ij} = \frac{\mu_0}{4 \cdot \pi} \cdot \frac{3 \cdot (x_{0j} - x_i)}{\rho_{ij}^5} \cdot (L_{ij}) - \frac{\mu_0}{4 \cdot \pi} \cdot \frac{mx_i}{\rho_{ij}^3} \tag{3}$$

$$By_{ij} = \frac{\mu_0}{4 \cdot \pi} \cdot \frac{3 \cdot (y_{0j} - y_i)}{\rho_{ij}^5} \cdot (L_{ij}) - \frac{\mu_0}{4 \cdot \pi} \cdot \frac{my_i}{\rho_{ij}^3} \tag{4}$$

$$Bz_{ij} = \frac{\mu_0}{4 \cdot \pi} \cdot \frac{3 \cdot (z_{0j} - z_i)}{\rho_{ij}^5} \cdot (L_{ij}) - \frac{\mu_0}{4 \cdot \pi} \cdot \frac{mz_i}{\rho_{ij}^3} \tag{5}$$

$$L_{ij} = mx_i \cdot (x_{0j} - x_i) + my_i \cdot (y_{0j} - y_i) + mz_i \cdot (z_{0j} - z_i) \tag{6}$$

and

$$\rho_{ij} = \sqrt{(x_{0j} - x_i)^2 + (y_{0j} - y_i)^2 + (z_{0j} - z_i)^2} \tag{7}$$

The total magnetic field in observation point j is then calculated as follows.

$$\vec{B}_j = \sum_{i=1}^{N} Bx_{ij} \cdot \hat{x} + \sum_{i=1}^{N} By_{ij} \cdot \hat{y} + \sum_{i=1}^{N} Bz_{ij} \cdot \hat{z} \tag{8}$$

2.2. PSO: A Short Overview

PSO is a relatively new stochastic evolutionary computation technique based on the movement and intelligence of swarms. Developed in 1995 by Kennedy and Eberhart [16], PSO based its ingenuity on the movement of a swarm of bees (particles)in a field. The particles' goal is to find the optimal location in a given search space. The particles begin in random points and are also characterized by random velocities. This process may be described as an initialization phase. The velocities change in every iteration of the algorithm taking into account both (i) the particle's personal and (ii) the swarm's global optimum. The particles' velocities depend on whether exploitation of the possible global optimum or exploration of the search space is predominant. The trade-off between exploring the search space and exploiting the possible optima is monitored by two factors denoting which option is ascendant. As the PSO algorithm unfolds and the particles explore the search space, the global and personal optima may be updated, resulting in updated velocities. Finally, the particles converge towards an optimum. The PSO terms and the corresponding entities are described below:

1. Particle or Agent: Each individual in the swarm. All particles start from random locations and move towards the directions of the (i) personal and (ii) global optimum.

2. Position: Position refers to a particle's place in the search space, represented by a (1×6) vector $\mathbf{D}$. Its elements represent the positions and magnetic moments of each dipole. Evidently, the elements of $\mathbf{D}_i$ are $(x_i,\ y_i,\ z_i,\ mx_i,\ my_i,\ mz_i)$, $i = 1, 2, \ldots, N$. This 6-dimensional space is the solution space for the problem being optimized, where any set of N vectors represents a solution to the problem. In the present work, the variable values that optimize the objective function need to be defined.

3. Fitness: In PSO, a function must be defined as a figure of merit of the adequacy of a position. This fitness function takes into account of all the dipoles positions in the solution space and returns a single number evaluating that position. In the present work, the fitness

function represents the rms between the calculated and measured magnetic field strengths. Evidently, in the present work, rms needs to be minimized.

4. *pbest*: The position ($\mathbf{D}_i$) with the lowest fitness value encountered by each particle is known as the personal best or *pbest*. At each iteration, as the agent moves through the search space, it compares the fitness value of its current location to that of *pbest*. If the current location has a lower fitness value, *pbest* is replaced with its current location.

5. *gbest*: The position ($\mathbf{D}_i$) with the lowest fitness value encountered by all particles is known as the global best or *gbest*. At each iteration, as the agent moves through the search space, it also compares the fitness value of its current location to that of *gbest*. If the current location has a lower fitness value, *gbest* is then replaced with its current location. Obviously, in each iteration there is only one *gbest*.

2.3. Applying PSO for MDM Problem

To formulate the MDM problem under consideration, a $(3 \times M)$ matrix **TBth** is created. Its elements correspond to the magnetic field values at the observation points $j = 1, 2, \ldots, M$. A $(3 \times M)$ matrix **TB** is defined to include the produced magnetic fields at each iteration. As the proposed scheme unfolds, each agent updates its position, and then its value is employed to update **TB** by using equations (1)–(8). The positions and velocities of the agents are originally randomly selected. After the evaluation of *pbest* and *gbest*, the particles' positions are updated as shown in (9) [16]. The velocity of the element i of dipole n, v_{in}, is calculated as follows:

$$v_{in} = w \cdot v_{in} + c_1 \cdot rand() \cdot (pbest_{in} - p_{in}) + c_2 \cdot rand() \cdot (gbest_i - p_{in}) \quad (9)$$

where w represents the scale of the previous iteration's velocity, and c_1 and c_2 are factors determining the trade-off between exploring the search space and exploiting the possible optimal solution. p_{in} represents the position of element k of dipole i (corresponding to the appropriate element of $\mathbf{D}_i$). In the present work after extended simulations, the appropriate values of the aforementioned factors are $c_1 = c_2 = 2$ and $w = 0.5$.

Then, the positions are calculated as follows:

$$p_{in} = p_{in} + v_{in} \quad (10)$$

As the proposed scheme unfolds, the particles' positions and velocities are updated, resulting in updating **TB**. Accordingly, a $(3 \times M)$ matrix **TBg** represents the total magnetic field produced by *gbest*, and a

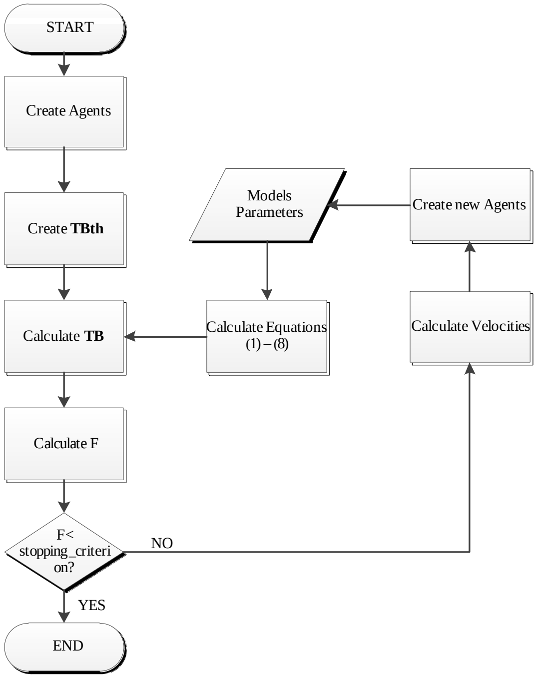

Figure 2. Flowchart of the proposed scheme.

$(3 \times M)$ matrix **TBp** represents the total magnetic field produced by *pbest*.

To evaluate the suitability of each solution, rms is used as the fitness function and defined as follows:

$$F = \sqrt{\frac{\sum_{i=1}^{N} \sum_{j=1}^{M} (TB_{ij} - TBth_{ij})^2}{N}} \tag{11}$$

Evidently, if a solution's fitness is lower than *pbest*, then *pbest* is replaced with the current solution, and *gbest* is possibly replaced too. The flowchart of the proposed scheme is depicted in Figure 2.

3. NUMERICAL RESULTS

In order to check the efficiency of the proposed method, a set of N dipoles was used to create a sample of the magnetic field in various points. This sample was created by using equations (1)–(8) comprising **TBth**. In each iteration of the proposed scheme, these so called "measurements" are used to estimate the models' positions and magnetic moments (hereafter referred to as models parameters). The models' parameters are used to update **TB**, as mentioned above, in order to equate its elements with the **TBth** elements.

Initially, these "measurements" (**TBth**) were produced based on one dipole, i.e.,

$$(x=-0.03,\ y=0.05,\ z=-4.05,\\ m_x=452.34,\ m_y=-484.63,\ m_z=-550.47);$$

Positions are measured in centimeters, and magnetic moments are measured in mAm^2. The proposed scheme, aiming at minimizing the aforementioned fitness function F, converges at the MDM represented by

$$\mathbf{D}_1 = (-0.03, 0.05, -4.0499, 452.3406, -484.627, -550.471)$$

Evidently, the proposed scheme was able to reconstruct the theoretical models parameters, since these values are practically identical.

To evaluate the proposed schemes' ability to create the correct MDM even in cases where the "measurements" are distorted by noise, each element of the original **TBth** was altered using a uniform distribution, as follows:

$$\mathbf{TBth}_{ij} = \mathbf{TBth}_{ij} + \mathbf{TBth}_{ij} \cdot (a \cdot rand() - a \cdot rand()) \qquad (12)$$

where α stands for the maximum distortion percentage of the "measurements". The proposed scheme was tested for two values for α, i.e., 1% and 5%. The models' parameters for the theoretical model and the MDM, produced by the proposed algorithm, for 1% and 5% distortion, are included in Table 1.

As readily observed by Table 1, as the percentage of the distortion increases, the divergence between the estimated MDM

Table 1. Comparison between the theoretical models parameters and the MDMs parameters, calculated by the proposed scheme, when $\alpha = 1\%$ and 5%.

	Theoretical	MDM 1%	MDM 5%
x (cm)	−0.03	−0.0158	−0.0146
y (cm)	0.05	0.0495	−0.0502
z (cm)	−4.05	−4.0476	−3.9933
mx (mAm^2)	452.34	452.9344	450.8042
my (mAm^2)	−484.63	−485.013	−483.137
mz (mAm^2)	−550.47	−550.608	−549.991

and the theoretical model increases too. However, the proposed scheme ameliorates the noises effects in the total magnetic field. The differences between the theoretical magnetic field values and the so

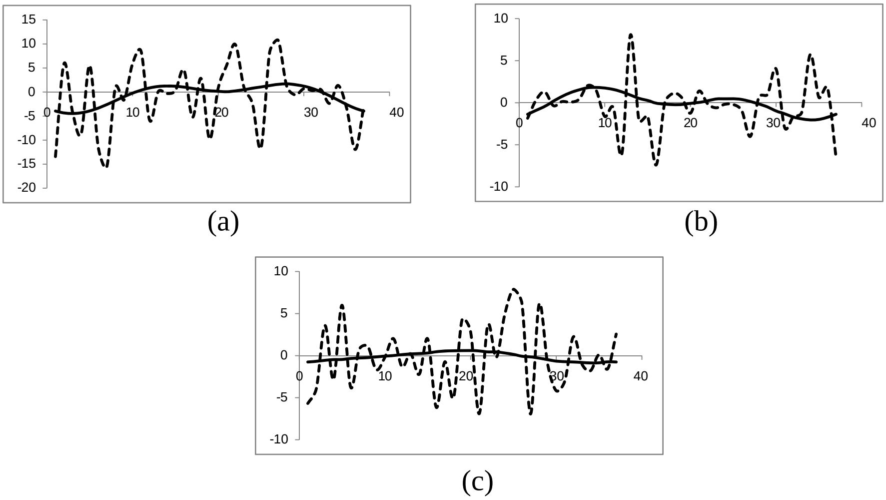

Figure 3. Differences between the theoretical magnetic field and the MDMs magnetic field for $\alpha = 1\%$. (a) x axis, (b) y axis, (c) z axis.

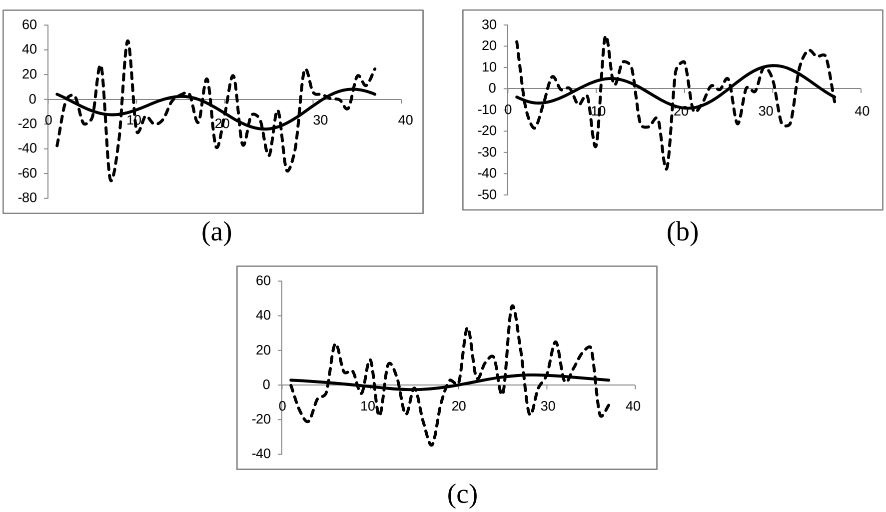

Figure 4. Differences between the theoretical magnetic field and the MDMs magnetic field for $\alpha = 5\%$. (a) x axis, (b) y axis, (c) z axis.

called "measurements" for 1% distortion are depicted in Figure 3 in dashed line, and the differences between the theoretical magnetic field values and the MDMs values are depicted in continuous line. The same differences for 5% distortion are depicted in Figure 4. Note, as expected, that the difference between the theoretical and the predicted values increases as the distortion percentage increases from up to 1% to up to 5%.

Afterwards, the proposed algorithms performance is evaluated by simulating a set of three dipoles to create a new **TBth**. The theoretical models' parameters used are tabulated in Table 2. In order to estimate the models' parameters from the new so called "measurements" (**TBth**), extended simulations were performed to find the minimum number of test points. The total number of the models' parameters to be estimated is eighteen, since the MDM is composed by three dipoles. Thus, theoretically, the number of test points needed to be examined is at least six. These test points must be carefully chosen in order to result in "independent" equations regarding to the parameters to be estimated. It is observed that the aforementioned test points instead of being positioned in a circle, as described in Section 2,

Table 2. Theoretical models parameters for a set of three dipoles.

	Theoretical Model		
	dipole 1	dipole 2	dipole 3
x (cm)	0.3	1	1.4
y (cm)	1.1	0.5	2
z (cm)	1.6	1.8	0.5
mx (mAm^2)	400	-500	600
my (mAm^2)	-400	500	-600
mz (mAm^2)	450	-550	450

Table 3. Calculated MDMs parameters when 3 dipoles are simulated.

	MDM		
	dipole 1	dipole 2	dipole 3
x (cm)	0.2487	1.0171	1.4131
y (cm)	1.2204	0.5908	1.9635
z (cm)	1.6019	1.7444	0.5067
mx (mAm^2)	374.1063	-494.799	619.9692
my (mAm^2)	-392.608	512.5497	-619.298
mz (mAm^2)	429.4842	-554.979	474.9911

is preferred to be located in symmetrical positions. Based on equations (1) to (8), it is observed that the set of test points is preferable to be in the dipoles' near field. In the present work, the test points (20, 0, 0), (0, 20, 0), (0, 0, 20), (15, 15, 0), (15, 0, 15) and (0, 15, 15) were selected. The results concerning the models estimation are tabulated in Table 3. As readily observed, the proposed scheme achieves an adequately accurate estimation of the theoretical model.

Since the proposed scheme is based on a stochastic approach, it is evident that the fitness function is needed to be minimized as much as possible. Three typical fitness function values are tabulated in Table 4. These values are characterized as good, mediocre and bad. As the

Table 4. Good, mediocre and bad fitness function values and the according MDM parameters.

Fitness (rms)		5.6667	
	dipole 1	dipole 2	dipole 3
x (cm)	0.2487	1.0171	1.4131
y (cm)	1.2204	0.5908	1.9635
z (cm)	1.6019	1.7444	0.5067
mx (mAm^2)	374.1063	−494.799	619.9692
my (mAm^2)	−392.608	512.5497	−619.298
mz (mAm^2)	429.4842	−554.979	474.9911
Fitness (rms)		26.5556	
	dipole 1	dipole 2	dipole 3
x (cm)	0.5495	1.3353	1.5443
y (cm)	1.5492	0.532	1.7487
z (cm)	1.2256	1.6128	0.561
mx (mAm^2)	402.3375	−498.134	593.2879
my (mAm^2)	−413.967	481.7637	−569.153
mz (mAm^2)	426.5415	−512.787	436.8797
Fitness (rms)		49.3333	
	dipole 1	dipole 2	dipole 3
x (cm)	1.8863	1.8044	1.0036
y (cm)	−0.2348	−0.4224	2.1399
z (cm)	0.2558	1.0537	0.5857
mx (mAm^2)	400.9172	−496.603	585.5265
my (mAm^2)	−355.013	475.6016	−623.263
mz (mAm^2)	454.1464	−537.38	441.9469

fitness function value decreases, the model's prediction is significantly more accurate.

In order to succeed in minimizing the fitness function value, extended simulations must be conducted to estimate the parameters bounds. This process is of crucial importance, since the convergence speed of the proposed scheme depends on the selected boundaries.

4. CONCLUSIONS

A stochastic based approach is proposed in the present work to create an efficient MDM based on a set of measurements employed. The proposed scheme is able to create an accurate MDM. A set of 1 or 3 dipoles were used to create these measurements for evaluation purposes. In the simulations presented, the proposed scheme was able to create an accurate MDM even in cases where the "measurements" were distorted by noise and to mitigate its effects.

REFERENCES

1. Mehlem, K., "Multiple magnetic dipole modeling and field prediction of satellites," *IEEE Transactions on Magnetics*, Vol. 14, No. 5, 1064–1071, Sep. 1978.
2. Nara, T., S. Suzuki, and S. Ando, "A closed-form formula for magnetic dipole localization by measurement of its magnetic field and spatial gradients," *IEEE Transactions on Magnetics*, Vol. 42, No. 10, 3291–3293, Oct. 2006.
3. Song, H., J. Chen, D. Zhou, D. Hou, and J. Lin, "An equivalent model of magnetic dipole for the slot coupling of shielding cavity," *8th International Symposium on Antennas, Propagation and EM Theory, ISAPE 2008*, 970–973, Nov. 2–5, 2008.
4. Junge, A. and F. Marliani, "Prediction of DC magnetic fields for magnetic cleanliness on spacecraft," *2011 IEEE International Symposium on Electromagnetic Compatibility (EMC)*, 834–839, Aug. 14–19, 2011.
5. Endo, H., T. Takagi, and Y. Saito, "A new current dipole model satisfying current continuity for inverse magnetic field source problems," *IEEE Transactions on Magnetics*, Vol. 41, No. 5, 1748–1751, May 2005.
6. Mehlem, K. and A. Wiegand, "Magnetostatic cleanliness of spacecraft," *2010 Asia-Pacific Symposium on Electromagnetic Compatibility (APEMC)*, 936–944, Apr. 12–16, 2010.

7. Mikki, S. M. and Y. M. M. Antar, "Near-field analysis of electromagnetic interactions in antenna arrays through equivalent dipole models," *IEEE Transactions on Antennas and Propagation*, Vol. 60, No. 3, 1381–1389, Mar. 2012.
8. Ciamak, A. and H. Jürgen, "Real-time ECG emulation: A multiple dipole model forelectrocardiography simulation," Studies in Health Technology and Informatics, 142:7_9, PMID: 19377101, 2009.
9. Pan, S., J. Kim, S. Kim, J. Park, H. Oh, and J. Fan, "An equivalent three-dipole model for IC radiated emissions based on TEM cell measurements," *2010 IEEE International Symposium on Electromagnetic Compatibility (EMC)*, 652–656, Jul. 25–30, 2010.
10. Zhang, Y.-J., S.-X. Gong, X. Wang, and W.-T. Wang, "A hybrid genetic-algorithm space-mapping method for the optimization of broadband aperture-coupled asymmetrical U-shaped slot antennas," *Journal of Electromagnetic Waves and Applications*, Vol. 24, No. 16, 2139–2153, 2010.
11. Wang, J., B. Yang, S. H. Wu, and J. S. Chen, "A novel binary particle swarm optimization with feedback for synthesizing thinned planar arrays," *Journal of Electromagnetic Waves and Applications*, Vol. 25, Nos. 14–15, 1985–1998, 2011.
12. Rahmat-Samii, Y., "Genetic algorithm (GA) and particle swarm optimization (PSO) in engineering electromagnetics," *17th International Conference on Applied Electromagnetics and Communications, ICECom 2003*, 1–5, Oct. 1–3, 2003.
13. Ali, F. A., K. T. Selvan, "A study of PSO and its variants in respect of microstrip antenna feed point optimization," *Asia Pacific Microwave Conference, APMC 2009*, 1817–1820, Dec. 7–10, 2009.
14. Nanbo, J. and Y. Rahmat-Samii, "Advances in particle swarm optimization for antenna designs: Real-number, binary, single-objective and multiobjective implementations," *IEEE Transactions on Antennas and Propagation*, Vol. 55, No. 3, 556–567, Mar. 2007.
15. Elgallad, A., M. El-Hawary, W. Phillips, and A. Sallam, "PSO-based neural network for dynamic bandwidth re-allocation [power system communication]," *2002 Large Engineering Systems Conference on Power Engineering, LESCOPE 02*, 98–102, 2002.
16. Kennedy, J. and R. Eberhart, "Particle swarm optimization," *Proceedings of IEEE International Conference on Neural Networks*, Vol. 4, 1942–1948, Nov./Dec. 1995.